



Oxygen-vacancy concentration in $A_2MgMoO_{6-\delta}$ double-perovskite oxides

Y. Matsuda^a, M. Karppinen^{a,b,*}, Y. Yamazaki^c, H. Yamauchi^{a,b}

^a Materials and Structures Laboratory, Tokyo Institute of Technology, Yokohama 226-8503, Japan

^b Laboratory of Inorganic Chemistry, Department of Chemistry, Helsinki University of Technology, FI-02015 TKK, Finland

^c Department of Innovative and Engineered Materials, Tokyo Institute of Technology, Yokohama 226-8502, Japan

ARTICLE INFO

Article history:

Received 7 February 2009

Received in revised form

13 April 2009

Accepted 16 April 2009

Available online 23 April 2009

Keywords:

Double perovskite

Oxygen content

Chemical substitution

Coulometric titration

SOFC anode material

ABSTRACT

Accurate oxygen-content analysis by means of a coulometric redox titration method specially devised for the purpose shows that as-synthesized (in 5% H_2/Ar) samples of the recently reported novel solid oxide fuel cells anode material $Sr_2MgMoO_{6-\delta}$ contain oxygen vacancies with a concentration of $\delta \approx 0.05$. Oxygen contents and the resultant Mo-valence values are also analyzed for various $A_2MgMoO_{6-\delta}$ samples in order to reveal both the isovalent and aliovalent A-site cation substitution effects.

© 2009 Elsevier Inc. All rights reserved.

1. Introduction

Solid oxide fuel cells (SOFCs) are capable of converting chemical energy of a fuel (e.g. hydrogen) directly and with a high efficiency into electricity. One of the desires yet to be realized is to develop anode materials for SOFCs that would operate properly not only with pure H_2 gas but also with low-cost and more abundant fuels such as natural gas [1–4]. The conventional choice for the anode material, Ni/YSZ cermet, gets readily poisoned by carbon and sulfur present in natural gas and other hydrocarbon-based fuels.

Recently Huang et al. [5,6] demonstrated that the B-site ordered double-perovskite oxide $Sr_2MgMoO_{6-\delta}$ tolerates well both carbon and sulfur and shows excellent SOFC-anode performances for a variety of fuels (though the phase stability under highly reducing conditions has been discussed [7,8]). A necessary requirement for a material to perform well as an SOFC anode is that it is a “mixed ion and electron conductor” (MIEC). In $Sr_2MgMoO_{6-\delta}$ the MIEC condition is apparently connected with the presence of oxygen vacancies which would not only give good oxide-ion conduction but also create mixed-valent $Mo^{VI/VI}$ species and hence result in good electron conduction [5,6]. Even though a proper amount of vacant oxygen sites is believed to be crucially important for the MIEC oxides, little attention has been paid to the

reliable determination of the absolute oxygen contents in $Sr_2MgMoO_{6-\delta}$ and related double-perovskite samples.

We have developed an accurate coulometric titration method for the precise oxygen-content and Mo-valence analysis of $Sr_2MgMoO_{6-\delta}$ -type samples. The results obtained thereof reveal that the $Sr_2MgMoO_{6-\delta}$ phase indeed is oxygen-deficient. Oxygen contents and the resultant Mo-valence values were moreover determined for various $A_2MgMoO_{6-\delta}$ samples to gain deeper understanding on both isovalent (Ca^{II} and Ba^{II} for Sr^{II}) and aliovalent (La^{III} for Sr^{II}) A-site cation substitution effects in this exciting system. Note that recently Ji et al. [9] reported enhanced SOFC characteristics for their La^{III} -for- Sr^{II} substituted $(Sr,La)_2MgMoO_{6-\delta}$ samples.

2. Experimental

Sample synthesis: Polycrystalline samples of $A_2MgMoO_{6-\delta}$ ($A = Ca, Sr, Ba, La$; see Table 1 for the exact compositions) were synthesized by an EDTA-chelation method [10]. Stoichiometric amounts of $CaCO_3$, $SrCO_3$, $BaCO_3$, La_2O_3 , MgO and $(NH_4)_6Mo_7O_{24} \cdot 4H_2O$ powders were dissolved in 1 M HNO_3 solution from which the metal ions were chelated with an EDTA/ NH_3 solution containing EDTA in 50% excess. After evaporating the solvent and burning the residue, the remaining ash was calcined in air first at $400^\circ C$ for 12 h and then at 800 – $1200^\circ C$ for 8 h. Finally the calcined powder was pressed into pellets and sintered at $1000^\circ C$ (at $800^\circ C$ for $(Sr_{1-x}Ca_x)_2MgMoO_{6-\delta}$ with $x = 0.375$ and 0.500) in a 5% H_2/Ar gas flow for

* Corresponding author at: Laboratory of Inorganic Chemistry, Department of Chemistry, Helsinki University of Technology, P.O. Box 6100, FI-02015 TKK, Finland. Fax: +358 9 462 373.

E-mail address: maarit.karppinen@tkk.fi (M. Karppinen).

Table 1
Crystal structure data and oxygen-content determination results for the $A_2MgMoO_{6-\delta}$ samples.

A	a (Å)	b (Å)	c (Å)	β (deg.)	V (Å ³)	δ	ν_{Mo}
Ba	5.719	8.086	5.716	89.96	264.3	0.04	5.92
Ba _{0.875} Sr _{0.125}	5.712	8.064	5.707	89.84	262.6	0.04	5.92
Ba _{0.125} Sr _{0.875}	5.650	7.914	5.609	89.59	250.8	0.05	5.90
Sr	5.611	7.885	5.589	89.81	247.4	0.05	5.90
Sr _{0.875} Ca _{0.125}	5.608	7.902	5.571	89.61	247.0	0.05	5.90
Sr _{0.750} Ca _{0.250}	5.606	7.860	5.568	89.62	245.4	0.06	5.88
Sr _{0.625} Ca _{0.375}	5.608	7.848	5.561	89.42	244.8	0.06	5.88
Sr _{0.500} Ca _{0.500}	5.590	7.835	5.539	89.50	242.6	0.07	5.86
Sr _{0.875} La _{0.125}	5.593	7.899	5.675	89.62	250.8	-0.03	5.81
Sr _{0.750} La _{0.250}	5.660	7.890	5.602	89.40	250.2	-0.13	5.76
Sr _{0.625} La _{0.375}	5.644	7.925	5.600	89.44	250.6	-0.17	5.59
Sr _{0.500} La _{0.500}	5.649	7.934	5.605	89.52	251.2	-0.32	5.64

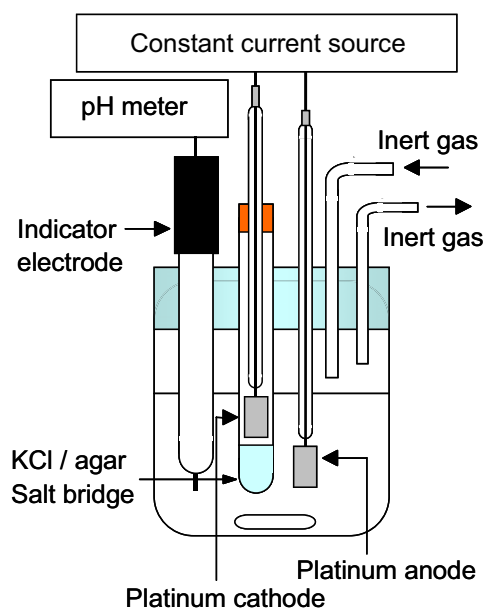


Fig. 1. Schematic illustration of the setup of the coulometric titration cell used in the present work.

24–48 h, followed by furnace-cooling in the same atmosphere. Note that the optimized calcination and sintering conditions were searched for each sample composition separately. X-ray powder diffraction data were collected for the samples (XRD; Rigaku RINT-2000 diffractometer equipped with a copper rotating anode; $CuK\alpha$ radiation) to confirm the phase purity and to determine the lattice parameters.

Oxygen-content analysis: All the samples were characterized for the precise oxygen content employing a coulometric titration technique originally developed for half-metallic $Sr_2FeMoO_{6-\delta}$ samples [11] and modified here for the present $A_2MgMoO_{6-\delta}$ samples. The technique is based on electrochemical oxidation of Mo^V and/or Fe^{II} species formed upon sample-dissolution in an acidic solution. Pentavalent Mo is not stable in the solution but most likely reduces Fe^{III} (if present) such that the species actually oxidized in the coulometric titration are not the Mo^V ions but rather an equivalent amount of Fe^{II} ions formed in the solution. Note that in the experiments reported in Ref. [11] for the $Sr_2FeMoO_{6-\delta}$ samples, the $Fe^{III/II}$ species are in-situ formed upon sample dissolution, whereas in the present case the $A_2MgMoO_{6-\delta}$ samples were dissolved in an acidic solution containing a known amount of Fe^{III} ions. The experiment was carried out as follows: an accurately weighed ~ 25 mg powder specimen of the

$A_2MgMoO_{6-\delta}$ sample was dissolved in 200 ml oxygen-free (by means of N_2 -gas bubbling) 3 M HCl solution containing an excess of Fe^{III} ions. The titration was carried out under N_2 -gas flow in order to prevent air-oxidation of the species to be oxidized electrochemically. The electrochemical oxidation of Fe^{II} (and Mo^V if present) was performed at a constant current of 1.5 mA until the potential against the Ag/AgCl electrode reached 820 mV [11], see Fig. 1 for the setup of the titration cell. The titration curves obtained for our $A_2MgMoO_{6-\delta}$ samples were essentially identical to that presented in Ref. [11] for $Sr_2FeMoO_{6-\delta}$. From the time required for the titration the quantity of electrons produced and thus the amount of Mo^V in the sample specimen (and the δ value in the $A_2MgMoO_{6-\delta}$ phase studied) could be calculated. For each $A_2MgMoO_{6-\delta}$ composition the titration experiment was repeated ten times to obtain the oxygen-content value $6-\delta$ with a reproducibility better than ± 0.01 (independent of the sample composition). Here it should also be mentioned that the Fe^{III} ions were generated in the solution prior to the sample-dissolution from ~ 5 mg $FeCl_2$ (dissolved in the solution) through electrochemical $Fe^{II} \rightarrow Fe^{III}$ oxidation performed with the same experimental parameters as those used for the coulometric titration proper.

3. Results and discussion

X-ray diffraction measurements revealed that phase-pure samples were reproducibly obtained within the entire substitution range for $(Sr_{1-x}Ba_x)_2MgMoO_{6-\delta}$ and up to $x = 0.5$ for the other two systems, $(Sr_{1-x}Ca_x)_2MgMoO_{6-\delta}$ and $(Sr_{1-x}La_x)_2MgMoO_{6-\delta}$, see the XRD patterns presented in Fig. 2 for representative samples. Lattice parameters were refined for all the samples in an acceptable manner from the XRD data in space group $P2_1/n$ [5,6,10], see Fig. 3 for the case of the

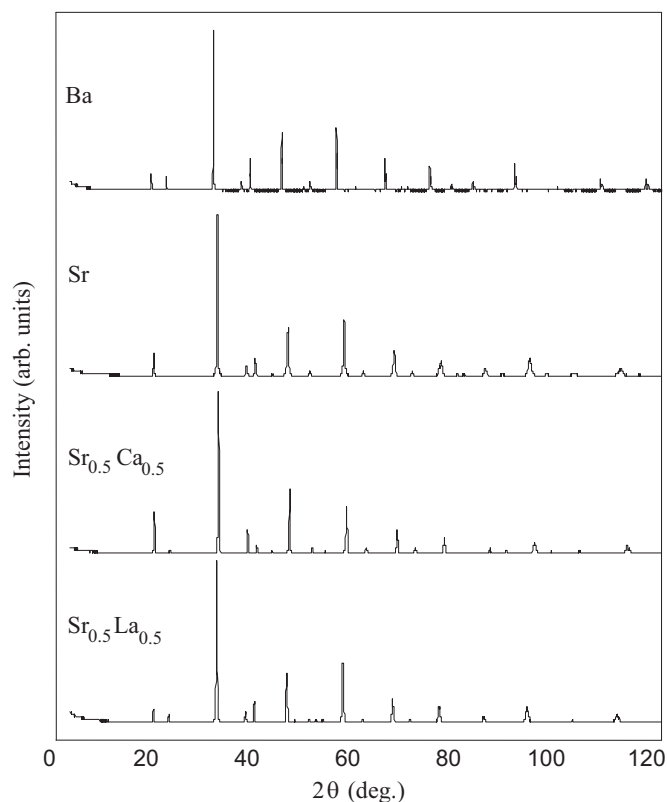


Fig. 2. XRD patterns for the $Ba_2MgMoO_{6-\delta}$ (top), $Sr_2MgMoO_{6-\delta}$, $(Sr_{0.5}Ca_{0.5})_2MgMoO_{6-\delta}$ and $(Sr_{0.5}La_{0.5})_2MgMoO_{6-\delta}$ (bottom) samples.

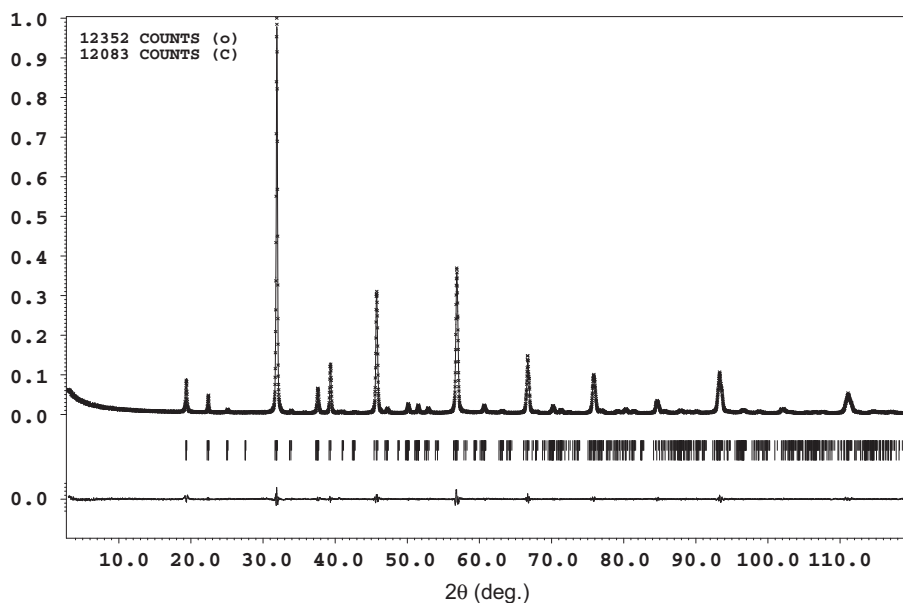


Fig. 3. Observed, calculated and difference XRD profiles from Rietveld refinement of data for the space group $P2_1/n$ (the ticks refer to the Bragg positions).

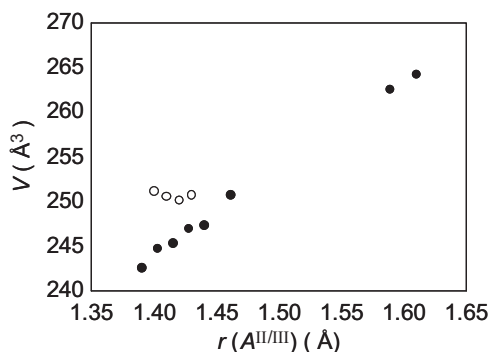


Fig. 4. Unit-cell volume plotted against the average ionic radius of the A-site cations for the isoivalent $(\text{Ba,Sr,Ca})_2\text{MgMoO}_{6-\delta}$ (●) and alioivalent $(\text{Sr,L a})_2\text{MgMoO}_{6-\delta}$ (○) samples.

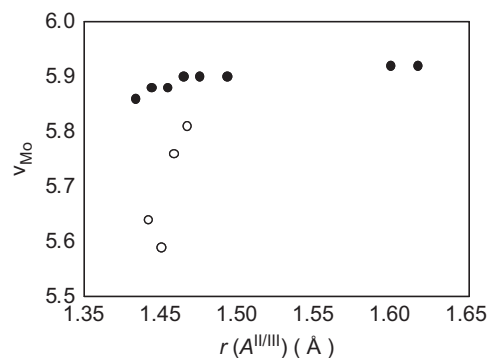


Fig. 5. Valence of molybdenum plotted against the average ionic radius of the A-site cations for the isoivalent $(\text{Ba,Sr,Ca})_2\text{MgMoO}_{6-\delta}$ (●) and alioivalent $(\text{Sr,L a})_2\text{MgMoO}_{6-\delta}$ (○) samples.

$(\text{Sr}_{0.5}\text{La}_{0.5})_2\text{MgMoO}_{6-\delta}$ sample. The results are summarized in Table 1. In Fig. 4 we plot the unit-cell volume V against the average ionic radius of the A-site constituent ions, $r(A^{II/III})$. For the divalent A-site constituents, V systematically increases with increasing $r(A^{II})$, as expected. Moreover seen from Fig. 2 is that in the $(\text{Sr,L a})_2\text{MgMoO}_{6-\delta}$ system gradual replacement of the larger Sr^{II} ions [$r(\text{Sr}^{II}) = 1.44 \text{ \AA}$] by the slightly smaller La^{III} ions [$r(\text{La}^{III}) = 1.36 \text{ \AA}$] does not decrease the size of the unit-cell but rather increases it. This may be attributed to the electron-doping effect, that is, a decrease in the valence state of molybdenum, ν_{Mo} , upon the alioivalent La^{III} -for- Sr^{II} substitution.

Results of the oxygen-content analyses are also summarized in Table 1. The original $\text{Sr}_2\text{MgMoO}_{6-\delta}$ phase is found oxygen-deficient as expected: for the present $\text{Sr}_2\text{MgMoO}_{6-\delta}$ samples synthesized in 5% H_2/Ar gas flow the δ value was determined at 0.05. Substitution of divalent Sr by the other divalent alkaline-earth elements did not change the situation strongly. However, careful inspection of the results obtained for the two sample series, $(\text{Sr,Ba})_2\text{MgMoO}_{6-\delta}$ and $(\text{Sr,Ca})_2\text{MgMoO}_{6-\delta}$, reveals a weak but systematic trend of increasing vacancy concentration (and decreasing ν_{Mo}) with decreasing $r(A^{II})$, from $\delta = 0.04$ ($\nu_{\text{Mo}} = 5.92$) for the $\text{Ba}_2\text{MgMoO}_{6-\delta}$ sample to $\delta = 0.07$ ($\nu_{\text{Mo}} = 5.86$) for the $(\text{Sr}_{0.5}\text{Ca}_{0.5})_2\text{MgMoO}_{6-\delta}$.

For the $(\text{Sr,L a})_2\text{MgMoO}_{6-\delta}$ system it was found that the alioivalent La^{III} -for- Sr^{II} substitution results in a gradual decrease in the valence value of molybdenum, ν_{Mo} (see Table 1). However, the decrease rate in ν_{Mo} is lower than that anticipated if the oxygen content is assumed to remain unaffected. In Fig. 5, we plot the valence value of molybdenum against the average ionic radius $r(A^{II/III})$ for all the presently studied $\text{A}_2\text{MgMoO}_{6-\delta}$ samples. With increasing La content x in $(\text{Sr}_{1-x}\text{La}_x)_2\text{MgMoO}_{6-\delta}$, the Mo-valence value decreases from $\nu_{\text{Mo}} = 5.9$ for $x = 0$ to $\nu_{\text{Mo}} \approx 5.6$ for $x > 0.3$. Provided that the oxygen content remains the same independent of the degree of the La^{III} -for- Sr^{II} substitution, the ν_{Mo} value should decrease below 5.0 for $x = 0.5$. Apparently, with increasing x in $(\text{Sr}_{1-x}\text{La}_x)_2\text{MgMoO}_{6-\delta}$ the oxygen content $6-\delta$ gradually increases to partially counterbalance the electron-doping effect on the valence state of molybdenum, see Table 1. Such a phenomenon is rather common among related perovskite oxide systems.

Finally we note from Table 1 that for the La-substituted samples oxygen-content values higher than 6.00 were obtained. These values should, however, not be taken literally as an indication of presence of interstitial oxygen atoms in these samples; it is well known that the perovskite framework allows oxygen vacancies but not oxygen interstitials. Hence the nominal oxygen surplus detected in the La-substituted samples should be understood as a presence of cation vacancies rather than oxygen

interstitials, cf. the $\text{LaMnO}_{3+\delta}$ or $\text{La}_{1-x}\text{Mn}_{1-x}\text{O}_3$ simple perovskite system [12].

4. Conclusion

In the present work we have developed a highly reproducible and sensitive redox analysis method which allowed us to accurately establish the oxygen-content/Mo-valence values for the promising new SOFC-anode material $\text{Sr}_2\text{MgMoO}_{6-\delta}$ and its A-site substituted derivatives. For all the $\text{A}_2\text{MgMoO}_{6-\delta}$ samples with divalent A-site constituents oxygen vacancies with a concentration δ ranging from 0.04 ($A = \text{Ba}$) to 0.07 ($A = \text{Sr}_{0.5}\text{Ca}_{0.5}$) were detected with a weak tendency of increasing δ with decreasing $r(\text{A}^{\text{II}})$. Also revealed was that upon the aliovalent La^{III} -for- Sr^{II} substitution the electron-doping effect is partially counter-balanced by an increase in the oxygen-to-metal content ratio.

Acknowledgments

The present work was supported by a Grant for R&D of New Interdisciplinary Fields in Nanotechnology and Materials Program

of MEXT of Japan and also by Tekes (no. 1726/31/07) and Academy of Finland (no. 126528).

References

- [1] E.P. Murray, T. Tsai, S.A. Barnett, *Nature* 400 (1999) 649.
- [2] S. Tao, J.T.S. Irvine, *Nature Mater.* 2 (2003) 320.
- [3] A. Atkinson, S. Barnett, R.J. Gorte, J.T.S. Irvine, A.J. McEvoy, M. Mogensen, S.C. Singhal, J. Vohs, *Nature Mater.* 3 (2004) 17.
- [4] J.B. Goodenough, Y.H. Huang, *J. Power Sources* 173 (2007) 1.
- [5] Y.H. Huang, R.I. Dass, Z.L. Xing, J.B. Goodenough, *Science* 312 (2006) 254.
- [6] Y.H. Huang, R.I. Dass, J.C. Denyszyn, J.B. Goodenough, *J. Electrochem. Soc.* 153 (2006) A1266.
- [7] C. Bernuy-Lopez, M. Allix, C.A. Bridges, J.B. Claridge, M.J. Rosseinsky, *Chem. Mater.* 19 (2007) 1035.
- [8] D. Marrero-Lopez, J. Pena-Martinez, J.C. Ruiz-Morales, D. Perez-Coll, M.A.G. Aranda, P. Nunez, *Mater. Res. Bull.* 43 (2008) 2441.
- [9] Y. Ji, Y.H. Huang, J.R. Ying, J.B. Goodenough, *Electrochem. Commun.* 9 (2007) 1881.
- [10] Y.H. Huang, J. Lindén, H. Yamauchi, M. Karppinen, *Chem. Mater.* 16 (2004) 4337.
- [11] T. Yamamoto, J. Liimatainen, J. Linden, M. Karppinen, H. Yamauchi, *J. Mater. Chem.* 10 (2000) 2342.
- [12] H. Okamoto, H. Fjellvåg, H. Yamauchi, M. Karppinen, *Solid State Commun.* 137 (2006) 522.